

# A WEARABLE SSVEP-BASED BRAIN-COMPUTER INTERFACE WITH OFF-THE-SHELF COMPONENTS

L. Angrisani<sup>1</sup>, P. Arpaia<sup>1</sup>, A. Esposito<sup>2</sup>, N. Moccaldi<sup>1</sup>, M. Parvis<sup>2</sup>

<sup>1</sup>Department of Electrical Engineering and Information Technology (DIETI), Università degli Studi di Napoli Federico II, Naples, Italy

<sup>2</sup>Department of Electronics and Telecommunications (DET), Politecnico di Torino, Turin, Italy

E-mail: pasquale.arpaia@unina.it

**ABSTRACT:** In this paper, a wearable Brain-Computer Interface is proposed. This BCI exploits a non-invasive single-channel electroencephalogram to measure steady-state visually evoked potentials (SSVEP) from the user's scalp. Dry electrodes are employed. The visual stimuli for SSVEP elicitation are presented on the LCD display of Augmented Reality glasses, and each stimulus can be associated with a command to actuate. The brain signals processing is conducted by means of a simple power spectral density analysis based on an FFT algorithm. Then, the signal features are classified with a Support Vector Machine. The resulting algorithm requires a low computational burden, and it was easily implemented in Android. The final BCI system is built with off-the-shelf components, and it is easily customizable. This work aims to give a contribution to the development of BCI systems for applications in daily life.

## INTRODUCTION

A Brain-Computer Interface (BCI) is a powerful tool capable of improving our way of communicating with the external world [1]. Historically, BCI applications have been addressed to help people with severe motor disabilities or other medical diseases [2, 3]. However, in the last decade, other fields have considered the adoption of a BCI, such as gaming, entertainment, education, or robotics [4–6], and today we are assisting to a rapid growth of this technology [7]. Nonetheless, the majority of work on BCI still remains at the level of laboratory research. The reasons for that are technical limitations, such as the problem of motion artifacts [8] or the trade-off between speed and performance of the BCI [9], and practical limitations, such as costs and wearability [10]. Aiming to build a wearable device to use in daily life, a non-invasive technique for brain activity measurement must be considered. Electroencephalography (EEG) is here taken into account. Indeed, EEG can be inexpensive and safe, while providing a spatial resolution in the order of centimeters and temporal resolution in the order of milliseconds [11]. Several paradigms there exist for BCI systems, such as motor-imagery [12, 13], P300 [14], or SSVEP [15–17]. In particular, “steady-state visually evoked potentials” (SSVEP) are highly reliable in

terms of accuracy and reproducibility [15, 18, 19] and user training is not mandatory [20, 21]. Hence, a SSVEP-based BCI is a suitable choice for a practical device.

In the present work, a single differential channel with dry electrodes is considered for the acquisition of EEG signals. The resulting BCI is highly wearable and low-cost. Clearly, this choice has some drawbacks, such as a low signal-to-noise ratio (SNR) if compared to more invasive techniques, where electrodes implanted inside the scalp guarantee higher SNR, and few information on brain activity due to the employment of a single channel. These drawbacks are mitigated if SSVEP signals are considered because they guarantee a good SNR with respect to other paradigms. However, an SSVEP-based BCI requires visual stimuli, namely flickering LEDs or icons on a display. A possible solution is the employment of the LCD displays of Augmented Reality (AR) glasses. They can be employed for stimulus presentation without affecting system wearability. The combination of BCI and AR platforms is not new. In [22], research solutions were surveyed, and it was highlighted that most state-of-the-art systems made use of two VEP-based paradigms, SSVEP or P300.

In a preceding phase, our research group demonstrated the feasibility of employing AR glasses in conjunction with a single-channel electroencephalography to build a wearable SSVEP-based BCI system. Moreover, the presented system has been built with components available off-the-shelf. The aim of the current work is to keep giving a contribution to the development of BCI systems that could be employed in everyday life. A particular focus is on the implementation of an algorithm for SSVEP signal classification. The remainder of this paper is organized as follows. The implementation of the system and the classification algorithm are first described. Then, the results of a training and evaluation procedure for assessing the performance of the SSVEP classifier are reported. Finally, the results are discussed and future steps addressed.

## MATERIALS AND METHODS

The architecture of the BCI system is here described, along with the off-the-shelf components employed for its implementation. The system of concern is divided into

three parts, (i) the visual stimuli generator, (ii) the EEG acquisition, and (iii) the signal processing.

As mentioned in the introduction, the stimulation consists of flickering icons on the LCD display of AR glasses. The Android-based “Epson Moverio BT-200” AR glasses were chosen (Fig. 1). These are relatively low-cost (about 600 € per unit) and provide the necessary characteristics for stimuli implementation. Notably, the 60 Hz refresh rate of the display allows for many flickering frequencies to be set. Two flickering icons were chosen as stimuli, at nominal frequencies equal to 10.0 Hz and 12.0 Hz, respectively. This choice is based on studies demonstrating that a good signal-to-noise ratio can be achieved at these frequencies [15], and this was also confirmed with some preliminary experiments. The AR glasses were programmed in Android Studio for the visual stimuli generation.



Figure 1: Epson Moverio BT-200 AR glasses.

The brain activity, containing the elicited SSVEP signals, is acquired with a non-invasive electroencephalography. A single differential channel consisting of two dry electrodes has been employed. These electrodes are placed on the user’s scalp according to the 10-20 system [23], at the points “Fpz” and “Oz”, as reported in Fig. 2. A third electrode is also needed as a ground. This electrode is usually placed on the forehead or ear location, but it can also be placed on a wrist or a leg [24].

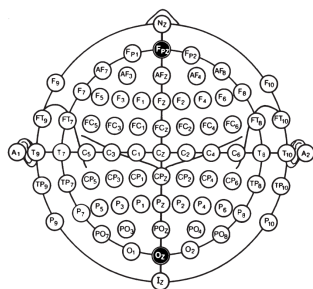


Figure 2: Placement of EEG electrodes in the International standard framework 10-20 [23] (in black): “Fpz” and “Oz”, in the scalp frontal and occipital region, respectively.

An open source EEG device, which is commercially available, was employed for the brain activity measurement, i.e. the Olimex EEG-SMT. This is shown in Fig. 3. Two active electrodes (CH1+ and CH1- respectively), and a passive electrode (DRL) are depicted too. The active

electrodes differ from the passive one because of some additional circuitry, based on operational amplifiers, for high-frequency interference rejection. These two electrodes were placed on the scalp, while the passive electrode was placed on the left wrist. The device and the electrodes total cost is less than 200 €. It is worth noting that the unused differential channel (CH2) was connected to the internal reference voltage as suggested by the EEG-SMT manual for achieving less noise. Fig. 3 also shows that some silver pins were soldered on one of the active dry electrodes. This electrode is placed on the occipital area (“Oz”), hence the pins aim to overcome the hair in order to better reach the user’s scalp.



Figure 3: Olimex EEG-SMT and dry electrodes.

The acquired EEG signal is converted from analog to digital thanks to the micro-controller being part of the EEG-SMT, and then it is continuously transferred through USB on a computing unit for elaboration. In this regard, the sampling frequency was set to 256 Sa/s, the A/D converter has a 10-bit resolution, and the overall gain was set to 6427 V/V. In the final integrated system, the digital EEG signal is directly transferred to the AR glasses micro-processor, where it is elaborated and the SSVEP signals classified. A command can then be associated to each class, namely the “10 Hz” class and the “12 Hz” class. However, to better study the signal processing, the EEG signal has been first transferred to a PC in order to be elaborated with MATLAB. After this step, whom results are reported in the following, the algorithm was ported in Android. A simple algorithm has been conceived, so that it could result in a low computational burden. This also means that the computational time does not affect the response time of the system, which is limited to some seconds because of the required stimulation/acquisition time. The signal time length is fixed within the algorithm. This acquisition time can be decided for each subject after an algorithm training phase, and it was initially fixed at 10.0 s for all the subjects.

The first processing step is a pass-band digital filtering. The pass-band has been set to (8-28) Hz so that the frequency components at the stimuli frequencies and their respective second harmonic are not corrupted. Meanwhile, the stop-band tries to reduce the effect of artifacts on the signal, especially EOG artifacts at low frequencies [25]. Note that, for example, a regression method

for artifact removal can not be employed aiming to adopt a single EEG channel. A FIR filter based on the Hamming windowing was designed. The order was set to 100, which resulted as a good compromise between computational burden and desired filter performance. The coefficients of the designed filter have been then employed for filtering in on-line signal analysis. After this step, the signal is zero-padded to the nearest power of 2 and transformed into the frequency domain with an FFT algorithm. In particular, the amplitude spectrum corresponding to the (8-28) Hz interval is derived, and the power spectral density (PSD) in the neighbour of the flickering frequencies can be calculated as signal features to be classified. For each stimulus frequency and their second harmonic, the power density is calculated as the sum of the squared amplitudes associated to corresponding bin and some nearest bins:

$$P(f_i) = \frac{1}{\Delta k} \sum_{n=k_i-\frac{\Delta k}{2}}^{n=k_i+\frac{\Delta k}{2}} A^2(n), \quad (1)$$

where  $k_i$  is the bin associated to the  $i$ -th frequency  $f_i$ ,  $\Delta k$  is the number of bins in the neighbour of  $k_i$ , and  $A(n)$  the amplitude associated to the  $n$ -th bin. In principle,  $k_i$  is found dividing  $f_i$  by the spectral resolution. However,  $f_i$  has an uncertainty due to the refresh rate frequency, which is not exactly 60 Hz. Hence, the algorithm automatically adjusts the  $k_i$  value looking for a peak (i.e. a maximum amplitude) in the neighbor of its initial value. This neighbor was chosen as the corresponding of a 0.5 Hz interval. Then, the  $\Delta k$  for the PSD calculation was chosen as the corresponding of a 0.2 Hz interval.

The last processing step is the SSVEP classification. In the present discussion, there are two features to take into account for each stimulus frequency (corresponding to a possible SSVEP frequency). The PSD corresponding to 10 Hz and 20 Hz are considered for the 10 Hz flickering icon, while the PSD corresponding to 12 Hz and 24 Hz are considered for the 12 Hz flickering icon. These pairs of PSD are classified with a simple machine learning supervised algorithm, the Support Vector Machine (SVM) [26]. Notably, a linear kernel was adopted and the SVM model was trained with experimental data from ten subjects consisting in labeled SSVEP signals. Then, further experimental data from the same subjects were employed for the SVM model evaluation, where the model is adopted to classify unlabeled signals. The details of this procedure are presented in the next section.

## RESULTS

Ten subjects, 5 males and 5 females between 22 and 29 years old, took part to the experiments. Each subject was asked to seat on a comfortable chair and limit unnecessary movements. Fig. 4 represents one of the subjects wearing the system. At this moment, the system is still a prototype, and the electrodes are placed with the help of tight bands.

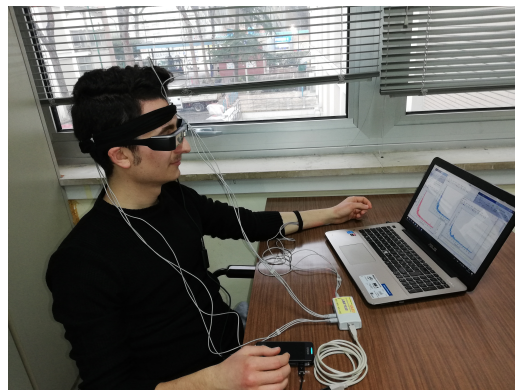


Figure 4: A subject wearing the BCI system during the experimental campaign.

In a first phase, signals were acquired for the training of the SVM model. Hence, the EEG-SMT was connected to a laptop with MATLAB. The laptop was disconnected from the AC power. At the beginning of each test, the raw EEG signal amplitude was checked in the frequency domain in absence of stimulation. A typical signal measured after wearing the EEG-SMT transducer is represented in Fig. 5. In this algorithm training phase, 12 trials were conducted. The brain signal was acquired for 10.0 s, with few seconds between consecutive trials. The subject could chose the icon to stare at, with the constraint that he/she had to choose 6 times 10 Hz and 6 times 12 Hz. The time the user had to stare at the icon corresponded to the acquisition duration, i.e. 10.0 s. Then, the subject declared the choice to the tester in order to assign a label to the trial. The features are extracted for these labeled data as explained in the previous section, and the labeled features are employed for the SVM training thanks to the MATLAB function 'fitsvm'. The classification accuracy of the trained model was then evaluated with 12 further trials. Labels were necessary for these signals too in order to compare the guessed labels with the actual ones. Moreover, several time windows were considered: with less samples of the signals acquired for 10.0 s, it was possible to analyze the classification accuracy with latencies from 2 s to 10 s. As already mentioned, a linear kernel was taken into account. The employment of a Gaussian ("rbf") kernel was also attempted, but a lower classification accuracy resulted. The classification accuracy obtained in the evaluation phase is reported in Tab. 1 for the ten subjects. It is to note that, in case of a single subject, one wrongly classified signal corresponds to an accuracy diminishing equal about to 8.3% (1/12). The mean classification accuracy is reported too in Fig. 6, where the accuracy of a random classifier is highlighted: since two classes (two stimuli) are considered, the accuracy of such a classifier is 50%.

## DISCUSSION

The trade-off between classification accuracy and latency has been considered. The usual trend is an accuracy diminishing when a shorter time window is taken into ac-

time [s]	S1	S2	S3	S4	S5	S6	S7	S8	S9	S10
2	100.0	100.0	58.3	83.3	91.7	83.3	91.7	91.7	50.0	66.7
3	100.0	100.0	91.7	91.7	100.0	83.3	91.7	91.7	50.0	58.3
4	100.0	100.0	91.7	58.3	91.7	91.7	91.7	66.7	50.0	58.3
5	100.0	100.0	100.0	91.7	91.7	91.7	91.7	75.0	91.7	75.0
6	100.0	100.0	100.0	91.7	91.7	91.7	91.7	83.3	83.3	66.7
7	100.0	100.0	100.0	91.7	100.0	91.7	100.0	75.0	91.7	58.3
8	100.0	100.0	100.0	91.7	100.0	100.0	100.0	83.3	83.3	58.3
9	100.0	100.0	100.0	83.3	100.0	100.0	91.7	100.0	83.3	75.0
10	100.0	100.0	100.0	83.3	100.0	100.0	91.7	100.0	83.3	83.3

Table 1: Classification accuracy of SSVEP signals for each subject (S1-S10) at varying time windows (2 s to 10 s).

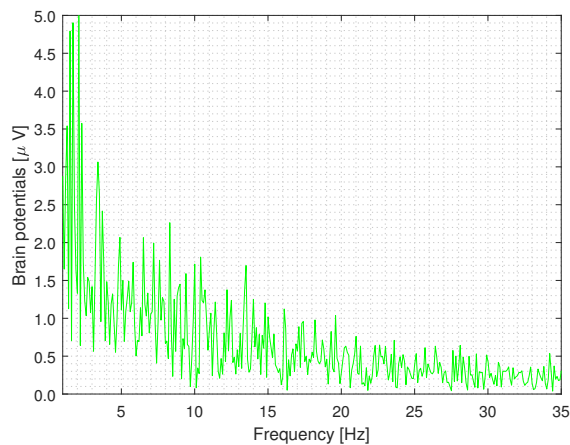


Figure 5: Amplitude spectrum of the raw EEG signal when the user is not stimulated.

count. In our case, the results of the experimental campaign show that, even with a BCI system built with components off-the-shelf and a simple signal processing, the accuracy is as high as 94% with a latency of 10.0 s, dropping to about 80% at 2.0 s. However, some exceptions in the accuracy trend are present depending on the subject. From one side, this could be explained with a varying attention level of the user during the stimulation time or the presence of artifacts localized in time, so that a longer time window is not necessarily better than a shorter one. On the other hand, these variations also depend on the adopted algorithm. Hence, it would be necessary to complicate the algorithm while trying to keep the computational burden low. The algorithm for SSVEP recognition should also be more robust with respect to artifacts. Nonetheless, it is worth noting that artifacts rejection could also be improved by enhancing the mechanical stability of electrodes placing. This implies that there is the need of a first level of engineerization for the adopted prototype.

These results are to be compared with other recent BCI-based systems proposed in literature. In [27], the employment of a single-channel BCI is proposed to build a speller. The user is stimulated for 10.0 s and the reported accuracy is 99.2%. This value was obtained considering 5 subjects. Another example is a speller based

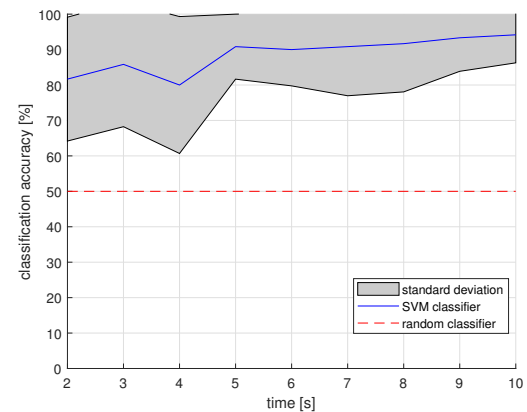


Figure 6: Mean classification accuracy of SSVEP signals calculated across 10 subjects at varying time windows.

again on a single-channel BCI and deep neural networks-based processing [28]. An example of solution integrating AR glasses and BCI is then reported in [29] for the control of a quadcopter. This system employs 14 dry electrodes and 2 reference electrodes, and the achieved accuracy was 85%, by considering 5 subjects executing a flight task. Hence, the performance of the system proposed in this manuscript are compatible with state-of-the-art results, though the system was built with off-the-shelf components.

Regarding the final system, it is possible to directly connect the EEG-SMT to the Moverio BT-200. In the Android application developed for the stimuli generation, the possibility to acquire the EEG data from USB and elaborate it was added. This was done to ensure the wearability of the system. However, it has been remarked there is still the need to investigate better signal processing algorithms prior to the porting of this algorithm in Android.

## CONCLUSION

A wearable BCI system with off-the-shelf components has been proposed. The BCI relies on SSVEP signals, elicited with flickering icons on AR glasses. It is easy to build such a system with relatively low-cost components as described within the paper, and applications are foreseen in daily life. As an example, the presented device is currently studied for an alternative communication channel with sensors in industrial or domotics applications. An important aspect that was treated is the classification algorithm. Signal features were extracted with a simple power spectral density analysis, and the PSD was calculated, for each icon, at the corresponding flickering frequency and its second harmonic. An experimental campaign was carried out to assess the classification accuracy for varying latencies. Classification was conducted with a Support Vector Machine.

Results demonstrated that the minimum stimulation and acquisition time for the SSVEP signals in our single-channel BCI can be as low as 2.0 s with mean accuracy equal to 80%, going up to 90.0% - 100.0% for some subjects. However, the need of further advances has been highlighted. Future research will deal with the optimization of the integrated system, enhancing the mechanical stability of electrodes placed both on the scalp and on the wrist, and moving on to wireless solutions to avoid the cumbersome wires that were needed in this prototype. An important performance increase is then expected with an improved algorithm, which should however remain enough "light" for an on-line EEG signal processing.

## REFERENCES

- [1] Wolpaw JR, Birbaumer N, McFarland DJ, Pfurtscheller G, Vaughan TM. Brain-computer interfaces for communication and control. *Clinical neurophysiology*. 2002;113(6):767–791.
- [2] Wolpaw JR et al. Brain-computer interface technology: a review of the first international meeting. *IEEE transactions on rehabilitation engineering*. 2000;8(2):164–173.
- [3] Schalk G, McFarland DJ, Hinterberger T, Birbaumer N, Wolpaw JR. BCI2000: a general-purpose brain-computer interface (BCI) system. *IEEE Transactions on biomedical engineering*. 2004;51(6):1034–1043.
- [4] Kerous B, Skola F, Liarokapis F. EEG-based BCI and video games: a progress report. *Virtual Reality*. 2018;22(2):119–135.
- [5] Perrin X, Chavarriaga R, Colas F, Siegwart R, Millán JdR. Brain-coupled interaction for semi-autonomous navigation of an assistive robot. *Robotics and Autonomous Systems*. 2010;58(12):1246–1255.
- [6] Sanchez-Fraire U, Parra-Vega V, Martinez-Peon D, Sepúlveda-Cervantes G, Sanchez-Orta A, Muñoz-Vázquez A. On the Brain Computer Robot Interface (BCRI) to Control Robots. *IFAC-PapersOnLine*. 2015;48(19):154–159.
- [7] Hu K, Chen C, Meng Q, Williams Z, Xu W. Scientific profile of brain-computer interfaces: Bibliometric analysis in a 10-year period. *Neuroscience letters*. 2016;635:61–66.
- [8] Minguillon J, Lopez-Gordo MA, Pelayo F. Trends in EEG-BCI for daily-life: Requirements for artifact removal. *Biomedical Signal Processing and Control*. 2017;31:407–418.
- [9] Spüler M. A high-speed brain-computer interface (BCI) using dry EEG electrodes. *PLoS one*. 2017;12(2):e0172400.
- [10] Penders J. Wearable, Wireless EEG Solutions in Daily Life Applications: What are we missing? *IEEE Journal of Biomedical and Health Informatics*. 2015;19:6–21.
- [11] Tan D, Nijholt A. Brain-computer interfaces and human-computer interaction. In: *Brain-Computer Interfaces*, 2010, 3–19.
- [12] Ahn M, Jun SC. Performance variation in motor imagery brain-computer interface: a brief review. *Journal of neuroscience methods*. 2015;243:103–110.
- [13] Lo C-C, Chien T-Y, Chen Y-C, Tsai S-H, Fang W-C, Lin B-S. A wearable channel selection-based brain-computer interface for motor imagery detection. *Sensors*. 2016;16(2):213.
- [14] Guger C et al. How many people are able to control a P300-based brain-computer interface (BCI)? *Neuroscience letters*. 2009;462(1):94–98.
- [15] Wang Y, Wang R, Gao X, Hong B, Gao S. A practical VEP-based brain-computer interface. *IEEE Transactions on Neural Systems and Rehabilitation Engineering*. 2006;14(2):234–240.
- [16] Ajami S, Mahnam A, Abootalebi V. Development of a practical high frequency brain-computer interface based on steady-state visual evoked potentials using a single channel of EEG. *Biocybernetics and Biomedical Engineering*. 2018;38(1):106–114.
- [17] Wang Y-T, Wang Y, Jung T-P. A cell-phone-based brain-computer interface for communication in daily life. *Journal of neural engineering*. 2011;8(2):025018.
- [18] Cheng M, Gao X, Gao S, Xu D. Design and implementation of a brain-computer interface with high transfer rates. *IEEE transactions on biomedical engineering*. 2002;49(10):1181–1186.
- [19] Volosyak I, Gembler F, Stawicki P. Age-related differences in SSVEP-based BCI performance. *Neurocomputing*. 2017;250:57–64.
- [20] Cecotti H. A self-paced and calibration-less SSVEP-based brain-computer interface speller. *IEEE Transactions on Neural Systems and Rehabilitation Engineering*. 2010;18(2):127–133.
- [21] Angrisani L, Arpaia P, Casinelli D, Moccaldi N. A Single-Channel SSVEP-Based Instrument With Off-the-Shelf Components for Trainingless Brain-Computer Interfaces. *IEEE Transactions on Instrumentation and Measurement*. 2018.
- [22] Si-Mohammed H, Argelaguet F, Casiez G, Rousset N, Lécuyer A. Brain-Computer Interfaces and Aug-

mented Reality: A State of the Art. In: Graz Brain-Computer Interface Conference. 2017.

[23] Klem GH, Lüders HO, Jasper H, Elger C, et al. The ten-twenty electrode system of the International Federation. *Electroencephalogr Clin Neurophysiol.* 1999;52(3):3–6.

[24] Teplan M et al. Fundamentals of EEG measurement. *Measurement science review.* 2002;2(2):1–11.

[25] Fatourehchi M, Bashashati A, Ward RK, Birch GE. EMG and EOG artifacts in brain computer interface systems: A survey. *Clinical neurophysiology.* 2007;118(3):480–494.

[26] Cortes C, Vapnik V. Support-vector networks. *Machine learning.* 1995;20(3):273–297.

[27] Ajami S, Mahnam A, Abootalebi V. Development of a practical high frequency brain–computer interface based on steady-state visual evoked potentials using a single channel of EEG. *Biocybernetics and Biomedical Engineering.* 2018;38(1):106–114.

[28] Nguyen T-H, Chung W-Y. A Single-Channel SSVEP-Based BCI Speller Using Deep Learning. *IEEE Access.* 2019;7:1752–1763.

[29] Wang M, Li R, Zhang R, Li G, Zhang D. A Wearable SSVEP-Based BCI System for Quadcopter Control Using Head-Mounted Device. *IEEE Access.* 2018;6:26789–26798.